Available online at www.sciencedirect.com

ScienceDirect

www.elsevier.com/locate/jes

JES JOURNAL OF ENVIRONMENTAL SCIENCES

www.jesc.ac.cn

Buoyancy and turbulence-driven atmospheric circulation over urban areas

Yifan Fan[1,*], **Julian Charles Roland Hunt**[1,2,3], **Yuguo Li**[1]

1. *Department of Mechanical Engineering, The University of Hong Kong, Hong Kong, China*
2. *Department of Earth Sciences, University College London, London, WC1E6BT, UK*
3. *Malaysian Commonwealth Studies Centre, Cambridge, CB23RF, UK*

ARTICLE INFO

Article history:
Received 26 November 2016
Accepted 23 January 2017
Available online 9 February 2017

Keywords:
Urban heat island
Buoyancy and turbulence-driven
Eddy structures
Atmospheric circulation
Pollutant dispersion

ABSTRACT

In the buoyancy and turbulence-driven atmospheric circulations (BTDAC) that occur over urban areas where the approach means wind speeds are very low (less than turbulent fluctuations and typically <3 m/sec), the surface temperatures are significantly higher than those in the external rural areas, and the atmosphere above the mixing layer is stably stratified. In this paper, the mechanisms of BTDAC formation are studied through laboratory experiments and modelling, with additional low-level inflow from external rural areas and a divergent outflow in the opposite direction in the upper part of the mixed layer. Strong turbulent plumes in the central region mix the flow between lower and higher levels up to the inversion height. There are shear-driven turbulent eddies and weaker buoyant plumes around the periphery of the urban area. As the approach flow is very weak, the recirculating streamlines within the dome restrict the ventilation, and the dispersion of pollution emitted from sources below the inversion height leading to a rise in the mean concentration. Low-level air entrained from rural areas can, however, improve ventilation and lower this concentration. This trend can also be improved if the recirculating structure of the BTDAC flow pattern over urban areas breaks down as a result of the surface temperature distribution not being symmetrical, or as the approach wind speed increases to a level comparable with the mean velocity of circulation, or (except near the equator) the urban area is large enough that the Coriolis acceleration is significant.

Introduction

Since cities were first established, their leaders and communities have worked in many different ways to understand and improve their natural and social urban environments. Several studies (*e.g.*, Eliasson, 2000; Hunt et al., 2005) have identified important differences in the urban atmospheric environment, such as whether the mean winds approaching the city are significant in relation to the magnitude of local turbulence. Typical of low latitude cities, the circulation is characterised by convergent inflow in the lower atmosphere and divergent outflow at a higher atmospheric level, with turbulent plumes rising up to the inversion or mixing height. Field data, experiments and numerical simulations show that in these quasi-static conditions, the depth of the mixing layer is greatest over the central part of the city (as in London; Hunt,

* *Corresponding author*. E-mail: u3002019@connect.hku.hk (Yifan Fan).

http://dx.doi.org/10.1016/j.jes.2017.01.009
1001-0742/

2005). This characteristic dome-shaped flow field is commonly referred to as buoyancy and turbulence-driven atmospheric circulation (BTDAC). Barlag and Kuttler (1991) and Eliasson and Holmer (1990) found that the background condition favoured by BTDAC occurs for about 10% of the year, but more so at low latitudes. The frequency of occurrence and amplitude of BTDAC in large cities can occur more frequently with different climatic and geographical conditions. Barlag and Kuttler (1991), Luo and Li (2011) and Wang and Li (2016) described the significant roles played by BTDAC in urban ventilation and urban planning. Fernando et al. (2001) proposed a new research focus on urban fluid mechanics to systematically examine fluid mechanics and contaminant dispersion in large cities.

Findlay and Hirt (1969) and Shreffler (1979) investigated urban-induced wind (also known as country breeze). However, only the convergent inflow in the lower atmosphere was detected and analysed; due to limitations on measurement, only the lower part of the BTDAC could be accessed.

The overall concept and modelling of BTDACs need improving, to account more thoroughly for the relation between the convergent flow near the urban centre but below the divergent outflow in the upper part of the mixed layer and below the inversion height, and the change in the turbulent structure from being shear dominated over the outer part of the urban area to plume dominated near the centre. Both these forms of large scale eddy motions interact and drive turbulent motions within the stratified inversion layer and also generate internal waves in the atmosphere above the inversion layer. The mean and turbulent flow vary over the day, evening and night, and has a significant effect of the diurnal variation of turbulent dispersion from local and area sources within and outside the urban area. The diurnal circulation also depends on the thermal properties of the buildings, and surfaces at and below the ground.

Recent research on BTDAC has included numerical simulations (*e.g.*, Ryu et al., 2013), field measurements (*e.g.*, Hidalgo et al., 2008b), reduced-scale models in air-tanks (*e.g.*, Noto and Okamoto, 1991), reduced-scale models in water-tanks (*e.g.*, Lu et al., 1997a; Moroni and Cenedese, 2015) and theoretical models (*e.g.*, Han and Baik, 2009; Hunt et al., 2012). The study of BTDAC mechanism can be used in pollutant concentration modelling in the urban area such as, Zhu et al. (2015), Long et al. (2016), Wang et al. (2015) and Yin et al. (2016).

1. Characteristics of BTDAC

1.1. Quasi-steady state during day-time and night-time BTDAC

The basic characteristics of a BTDAC over an urban area with a symmetrical distribution of surface temperature are illustrated in Figs. 1 and 2.

BTDAC consists of a convergent inflow at a lower atmospheric level, a divergent outflow at a higher level and a dome-shaped flow field resulting from entrainment and overshoot at the top of the BTDAC (Fig. 1). It is influenced by the following factors: (1) differences in heat flux between urban and rural areas; (2) background stratification, which is indicated by buoyancy frequency, *N*; and (3) urban morphology, such as the diameter of the built up region of the urban area (*D*), the roughness of the urban area (defined by z_o), building-area density and building frontal area density. During both the day, evening and the night, BTDAC is caused by a significant temperature difference between urban and rural areas. The turbulence structure depends significantly on the thermal properties of buildings and surface materials, as well as the interactions with the stable interface and the incoming rural flow.

Urban dome size determines the upper level of pollutant dispersion, as discussed in Section 4. As the energy balance in urban and rural areas varies diurnally, if the background wind speed is small, the overall BTDAC occurs over the same time scale. The force driving BTDAC is the buoyancy generated by a temperature difference between urban and rural areas. BTDAC is also affected by the magnitude and distribution of surface roughness elements, radiative exchanges with the buildings and other surface elements, and heat and momentum fluxes at the stably stratified inversion layer.

The magnitude of the self-generated BTDAC can be estimated from the overall thermal and kinetic energy balance of the atmosphere below the inversion layer, if the following assumptions are made: (1) the energy change caused by background wind is omitted; and (2) BTDAC is, for a certain period during the diurnal cycle, in a steady state, with no significant time variations of the velocity field or temperature field.

The resulting energy balance is described in Eq. (1) below:

$$E_u = E_{tur} + E_{diss} + E_r \tag{1}$$

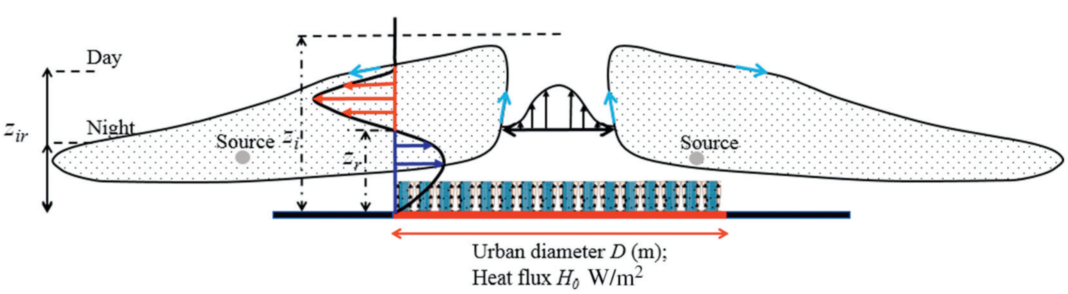

Fig. 1 – Schematic diagram of BTDAC for a two-dimensional or axisymmetric surface heating. Note that the differences in the mixing heights between the central (z_i) and external regions (z_{ir}) are larger in the evening and at night than during the day. The mean inflow is primarily driven by buoyant thermal forcing by day and by a shallow thickness gravity-current in the evening, driven inwards by the cool air from near the periphery. Also note the variation of the turbulence structure within and above the mixed layer, illustrated in Fig. 2. BTDAC: buoyancy and turbulence-driven atmospheric circulations.

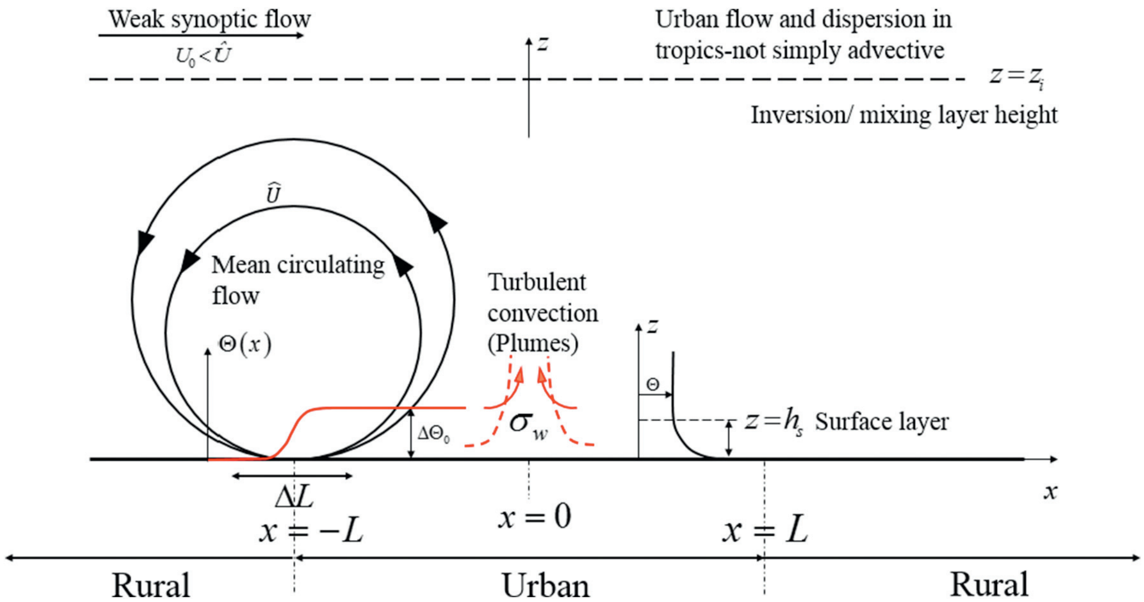

Fig. 2 – A simplified model for mean circulating flow $\hat{U}$ in the edge region driven by the strong gradient in thermal convection ($\hat{U} \approx \sigma_w > U_0$) over a horizontal distance ΔL. x and z are the horizontal and vertical coordinates respectively. σ_w is the standard deviation of the vertical velocity. U_0 is the synoptic wind speed. Θ represents potential temperature. $\Delta\Theta_0$ is the overall potential temperature jump between the urban center and the rural area. L is the radius of the urban area. h_s and z_i are surface layer height and mixed height respectively. The red solid curve represents the temperature difference profile across the horizontal distance ΔL in the urban edge region. The red dash line and arrows illustrate the thermal plumes. Note that the inward and outward shear flows shown in Fig. 1 are stimulated by this recirculation at the edge region.

where E_u is the energy supplied by the urban (anthropogenic heat flux and surface sensible heat flux). E_{tur} is the energy exchange at the dome boundary due to turbulence. E_{diss} is the energy dissipated due to the viscosity and friction. E_r is the energy released in the rural area (negative sensible heat flux in the rural area due to radiative cooling in the rural surfaces).

Previous researchers have described the horizontal extension of the urban dome at different times of the day and night, as summarised in Table 1.

Table 1 – A summary of the reported horizontal extensions of BTDAC.

Reference	Dome size	Dome time	Frequency of occurrence	Further remarks
Ryu et al. (2013)	The horizontal extension is approximately three times the size of the city.	17:30 Local Standard Time (LST)		Computational fluid dynamics (CFD) simulation; city size 20 km.
Lemonsu and Masson (2002)	Breeze extends horizontally for more than 50 km beyond the city centre.	Afternoon		CFD simulation; Paris simulated with a 20–30 km diameter.
Eliasson and Holmer (1990)	The BTDAC extends 40–70 m in the vertical direction and 20–26 km in the horizontal direction.	Night-time	Approximately 10%	Field measurements; city diameter approximately 10 km; if background wind >3 m/sec, no BTDAC observed.
Barlag and Kuttler (1991)			About 10%	Field measurement
Ganbat et al. (2014)	Horizontal extension at 13:00 (19:00) LST is 2.0 (3.9) times the size of the city.	Day-time		Urban diameter 20 km.
Hidalgo et al. (2008a)	Twice the diameter of the city (Toulouse, France).	Day-time (12:00–18:00)		CFD simulation
Hidalgo et al. (2008b)	Two to three times larger than the city.	Day-time (12:00–18:00)		Field measurement; urban breeze increases in intensity from 2 m/sec at 12:00 Coordinated Universal Time (UTC) to 5–6 m/sec at 18:00 UTC.

BTDAC: buoyancy and turbulence-driven atmospheric circulations.

Bohnenstengel et al. (2011) and Hunt et al. (2012) reported similar results as those in Table 1 on the horizontal extension of mean circulations.

Estimates and models of the mixed height z_i of BTDAC at the urban centre were proposed by many authors, including Catalano et al. (2012), Cenedese and Monti (2003), Kristóf et al. (2009), Moroni and Cenedese (2015) and Yoshikado (1992). An approximate consensus was that the mixed height at the urban centre, z_i, can be expressed in the form of Eq. (2), as follows:

$$z_i/D = A\mathrm{Fr}, \tag{2}$$

where A is a constant determined from experiments, $\mathrm{Fr}=u_D/ND$ is the Froude number. u_D is the scale of the horizontal component of the mean and eddying velocity as defined by $(g\beta H_0 D/\rho c_p)^{1/3}$ where H_0 is the surface heat flux in the urban area), N is the background buoyancy frequency and D is the urban diameter. g is the gravity acceleration. β, ρ and c_p are the thermal expansion rate, density and thermal capacity of the fluid.

1.2. Diurnal variations of the structure of BTDAC

However, the mixing height z_i and the overall circulation BTDAC vary in space and time between rural and urban regions and during the diurnal cycle. Typically during the day convective motions driven by solar radiation and the value of z_i (with typical values of 1–3 km) are broadly similar between rural and urban regions (with differences depending on the surface and building characteristics), with convective cells in the central area and roll structures and less intense turbulence associated with mean shear in the periphery (Falasca et al., 2013; Ryu et al., 2013). The gradients in the large scale turbulence drive the mean circulation – with the maximum inwards and outward radial mean velocity driven by the gradients in turbulence (Fan et al., under review).

The mean horizontal-velocity scale for these BTDAC flows in the day-time, U_d, is determined by H_u-H_r is the difference in surface heat flux between the urban and rural areas and by the mixed height in the urban area z_i, which was proposed by Hidalgo et al. (2010) and is shown in Eq. (3).

$$U_d = \left[g\beta z_i(H_u - H_r)/\rho c_p\right]^{1/3}, \tag{3}$$

Note that U_d is the maximum velocity scale near the periphery of the urban area and also is assumed to be large compared to the mean velocity U_o of the approach wind outside the urban area.

In the evening and during night-time periods large differences develop between urban and rural flow structure of the mean flow and turbulence. Typically in rural areas, z_i decreases to less than 100 m in the early evening with the cool air moving near the surface towards the central area. (*e.g.*, Hunt et al., 2012). At the same time over the central region of the city, the mixing height z_i remains much larger than in the rural value until late in the evening when it decreases to about 200 m (*e.g.*, Xie et al., 2013). During the quasi-steady night-time period the mean temperature gradient below the inversion is generally weakly stable, as a result of advection of cool air from rural areas, and interactions with the inversion layer.

An estimate of the velocity scale of the mean BTDAC at evening/night periods, U_n, which was proposed by Lu et al. (1997b), is given in Eq. (4).

$$U_n = \left(g\beta D H_0/\rho c_p\right)^{1/3} \tag{4}$$

where g denotes gravitational acceleration, β is the thermal expansion rate, D is the diameter of the urban area, H_0 is the difference between the surface heat fluxes for the urban and rural area, ρ denotes fluid density and c_p is fluid heat capacity.

Note that the velocity scale in the day-time U_d and the velocity scale in the night-time U_n are different as different length scales and heat fluxes are used.

This is approximately equivalent (Hunt et al., 2012) to the inflow gravity current U_{gc} from the rural to urban areas, which is expressed as Eq. (5).

$$U_{gc} \sim 0.6(g\beta z_i \Delta T)^{1/2} \tag{5}$$

where ΔT is the temperature difference between the urban area and the adjacent rural area.

This is also the approximate speed of the front, which shows that the time of evening transition over the whole urban area is of order D/U_{gc} (*i.e.* 3–5 hr for large cities of order 30 km radius). Note that the height of the mixed layer in the central region can remain as high as 500–1000 m which is significantly greater than that in the rural and outer urban areas. Thereafter during the quasi-steady night-time period, in BTDAC there is a lower urban mixed layer height z_i which is of order 200–300 m and a weaker mean circulation.

1.3. Coriolis effects in BTDAC in urban areas in temperate and subtropical latitudes

For mega cities in temperate and subtropical latitudes, the inflow in the lower part of the mixed layer is deflected by the Coriolis acceleration, which generates a mean velocity V_f in the cyclonic direction parallel to the periphery of the urban area.

During the day and night-time periods when the eddy motions and mean circulation are in an approximately steady state, the dynamics governing V_f is the balance between the Coriolis acceleration and the gradients of eddy stresses, with magnitude shown as Eq. (6) near the periphery.

$$V_f \sim fU_o/\left(\nu_e/z_i^2\right) \tag{6}$$

where ν_e is the eddy viscosity in the mixed layer which is stronger by day than that by night. f is the Coriolis parameter. Typically V_f is of order 1 m/sec for a large urban area. Since in most situations there is a weak mean flow U_o outside the urban area, the deflected Coriolis flow, as shown in Fig. 3 extends in the wake downwind of the urban area (Cheng and Chan, 2012).

In the transitional evening period for large urban areas, Coriolis acceleration deflects the gravity current in a cyclonic direction. The typical magnitude of V_f is of order 1 m/sec (Hunt and Simpson, 1982). The dynamics of typical unsteady urban gravity current with Coriolis differ significantly from

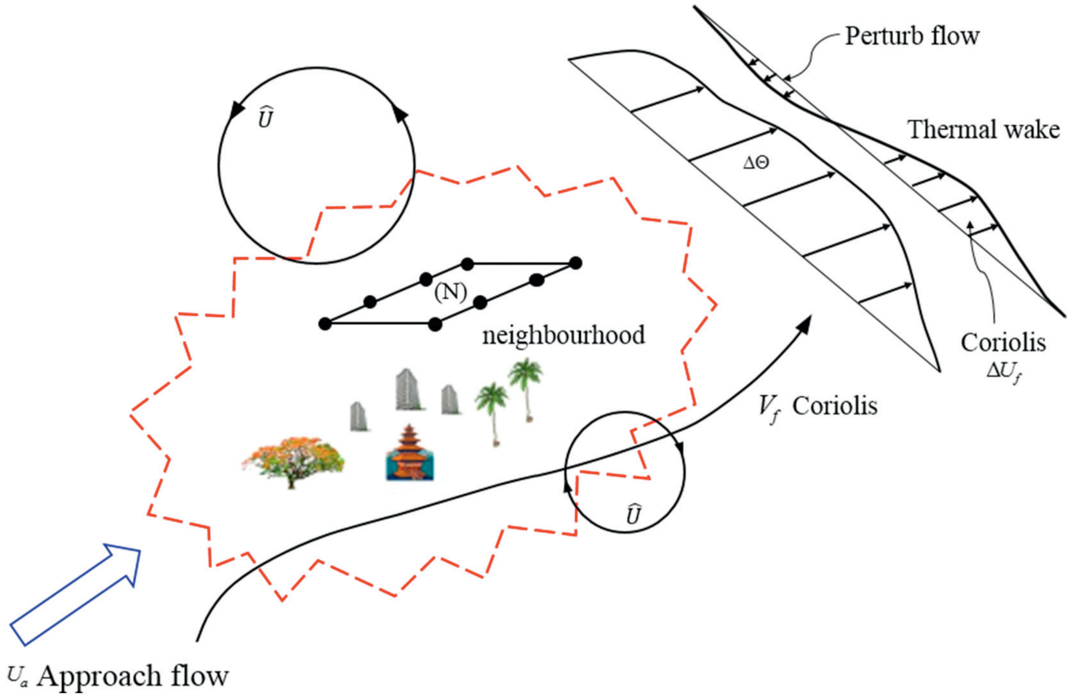

Fig. 3 – Streamlines and flow arrows to show the Coriolis effect on BTDAC in the northern hemisphere. $\hat{U}$ and U_a denote the mean circulating flow and the approach flow respectively. V_f is deflected velocity due to the balance between the Coriolis force and the gradient of eddy stresses. $\Delta\Theta$ is the overall potential temperature jump between the thermal wake region and the ambient rural area.

the larger synoptic scale weather fronts that travel over periods of order 1/*f* (Hunt et al., 2004, 2005).

2. Experimental and modelling studies of BTDAC

Physically-based theoretical conceptual models and reduced-scale models in laboratory experiments simplify the problem and enable researchers to identify the main physical dynamics of BTDAC. These apply in certain ideal conditions and with ideal geometries. They can produce reliable results and enable quantitative analysis of various factors, but scaling is always an issue, and it is difficult to model the rotation effect on a reduced-scale. Computer simulations in conjunction with the above methods provide an effective method for the quantitative and qualitative description of realistic urban environments.

New measurement data, which now include Lidar, tower data and high resolution satellite mapping of surface temperature as well as conventional meteorological surface variables, provide realistic descriptions over urban and rural areas, in particular the main spatial and time dependent features of BTDAC (*e.g.* as reviewed in Hunt et al., 2016). They accurately represent the real situation, and are able to identify structures and mechanisms determining the flow and thermal distributions. Compared with the other methods, field measurements also incur the highest costs and require the most labour and time. Furthermore, boundary and background conditions cannot be controlled when taking field measurements.

2.1. Mathematical analytical models

Lu et al. (1997b) proposed a hydrostatic model used to obtain the mean horizontal-velocity scale by solving the bulk-continuity, momentum and energy-conservation equations. The horizontal-velocity profile was obtained by solving a momentum equation with proper boundary conditions. Linear models provide another means of treating and solving governing equations. In essence, linear methods entail the linearization of governing equations with the assumption of minor perturbation. The governing equations are integrated into one equation to describe the flow field with proper boundary conditions. A stream function is used to reduce the number of unknown parameters in the momentum equation, and Fourier transform is performed to solve the equation. Vukovich (1971) used linear models to obtain a vertical cross section flow field. Mori and Niino (2002) used non-linear scaling to explore the evolution of BTDAC over time. The development of the flow was classified into three regimes: a turbulent diffusion regime, a low-level gravity-current regime and a gravity-wave regime above the mixing height.

If the temperature difference is significant for a long enough radial distance, the BTDAC is affected by the Coriolis force, which limits the horizontal extension of the circulation to achieve a thermal wind balance, as described in Section 2.3.

2.2. Field measurements

Field measurements are the most direct way of investigating flow fields over urban areas and in the urban canopy layer.

Snyder (1981) provided guidelines for the experimental design of field studies, and data collection and measurement points. However, it is difficult to extract specific flow characteristics from field measurements, which represent a combination of all of the physical processes occurring in and close to the urban area under study. It is crucial for researchers to be aware of all of the possible physical processes taking place during data acquisition and to implement suitable data-processing methods to obtain meaningful and reasonable results from field data. Statistical methods and tools have been used to investigate BTDAC in early field studies. For example, Barlag and Kuttler (1991), Eliasson and Holmer (1990) and Shreffler (1979) combined field measurements with numerical simulation for mutual validation. All of the field measurements reported in the studies above confirmed that BTDAC occurs during both day and night, and indicated the importance of BTDAC to urban ventilation and pollutant dispersion.

2.3. Reduced-scale models

2.3.1. Air-tank models

Noto and Okamoto (1991) first visualised BTDAC using an interesting fumigation method with a reduced-scale air-tank model. The urban area was assumed to be a two-dimensional heated strip-source. An overall qualitative description of the circulation phenomena BTDAC was proposed. The fumigation-based visualisation method and measures were later refined by Noto (1996). Using an air-tank model, different shapes and time dependence of the convective structures were shown to vary between quasi-steady, large scale plumes for low heat flux and high stratification above BTDAC, and unsteady smaller scale plume/puffs at high heat flux and low stratification. The latter structure is also associated with low thermal capacity and low thermal conductivity of the ground surface (Hunt et al., 2003).

Although a line source generated plume is fundamentally different from an area source generated plume, BTDAC is actually an example of the latter, with a large aspect ratio; see Fan et al. (2016a), the pioneering work done by Noto and Okamoto (1991) and Noto (1996) provided new insights into BTDAC and methods of modelling BTDAC.

In air-tank experiments, it is difficult to ensure the non-dimensional parameters required for similarity between the model and the 'prototype' atmospheric circulation patterns, such as the Froude number, the Reynolds number and the Rayleigh number. As temperature changes rapidly after the heater is turned on, due to the small thermal storage capacity of air, it is also difficult to temporally define the quasi-steady state, and the high temperatures may violate the Boussinesq approximation. Due to these disadvantages, water-tank reduced-scale models are increasingly favoured over air-tank experiments.

2.3.2. Water-tank models

Water-tank models are the reduced-scale models most widely used to simulate BTDAC. They can be quantitatively compared with prototype BTDAC patterns in the atmosphere. Lu et al. (1997a) first visualised BTDAC in water-tank experiments using the shadowgraph technique. The temperature field was measured using the thermal couple and the velocity field was analysed by image processing. The scaling parameters for temperature, velocity and length were selected to match the flow in the water-tank models with that in the atmosphere. The experimental results agreed well with the results of the numerical simulation, the theoretical mathematical models and the field measurements, indicating that water-tank models provide an effective and accurate means of simulating BTDAC. In research on the characteristics of BTDAC, Cenedese and Monti (2003), Falasca et al. (2013) and Moroni and Cenedese (2015) combined the use of water-tank models with new measurement techniques such as particle tracking velocimetry and feature tracking. Stable stratification can be achieved using either the heating method or the salt-water method.

Water-tank models can, however, also have limitations. (1) The process changes with time rather than being in a quasi-steady atmosphere; if heating continues and no heat sinks are present, the dome size will continue to increase during the experiment. However, the real physical processes in the atmosphere include radiative cooling in the rural area and at the top of the BTDAC. It is also difficult to simulate cooling in water-tank experiments. (2) The analogy with real BTDAC is limited by the size of the water-tank. The Reynolds number, Rayleigh number and Froude number of the modelled BTDAC differ from those of the real BTDAC. (3) Heat flux is uniform in laboratory-based water-tank experiments, which is not the case in reality. (4) Existing water-tank models (*e.g.*, Cenedese and Monti, 2003; Moroni and Cenedese, 2015) do not accommodate the drag caused by the urban canopy layer.

3. Dispersion in BTDAC

The diurnal variations in the mean and turbulent flows in BTDAC, described above, and the form (*e.g.*, local steady sources *Q* or finite mass sources *M*) and locations of sources (Xs, Ys and Zs) determine the patterns of dispersion over urban and adjoining rural areas. The dispersion is particularly affected by recirculating mean streamlines, intense turbulence and mean shear (Turfus, 1986, 1988); in these urban regions with diameter *D* and urban mixing depth z_i, if there is a mean steady source Q, then the mean concentration *C* increases with time (*i.e.*, $C \sim Qt/(z_i D^2)$); but because the streamlines also recirculate weakly outside the urban area, *C* also increases slowly in the surrounding rural area. The growth of concentration over large urban areas during weak synoptic external winds has been observed by Banta et al. (1998), Liang and Keener (2015), Masson et al. (2008), Miao et al. (2015), Parkhi et al. (2016) and Sini et al. (1996) and results in high levels of pollution. These events occur in both summer and winter in subtropical cities such as Beijing, for example. They previously only occurred in winter periods in large temperate zone cities, such as London, but now occur in summer in northern Europe and Russia.

If a finite volume or mass *M* is released, *e.g.*, over a large industrial area, then for a symmetric distribution of surface temperature, the pollutant is well mixed by the turbulence and shear, and the resulting average concentration over the urban area, C, is approximately constant for a period of the mean circulation. After a longer time period, the concentration *C* decreases as external rural air is entrained. However, if the surface temperature is asymmetrically distributed relative to the maximum temperature zone (Fan et al., under review), the ventilation can be much faster. If the central regions of the sources are located outside of the urban areas, the mean convergent inflow features into these BTDACs are particularly important.

4. Discussion

It is clear that each of the various methods of studying the BTDAC has its merits and weaknesses. Therefore, different methods in studying BTDAC may be used in combination. For example, mathematic models can be used to identify the important physical parameters. The scaled water-tank models and numerical simulations can be then used to quantitatively obtain the flow structures (mean velocity and temperature field, plumes structures and turbulent statistics) and scaling constants. The theoretical and reduced-scale experimental models can be verified by the field measurements. It would be difficult to obtain the whole velocity field to visualise the BTDAC through the field measurements due to the limitation of the available measurement techniques over such a large scale. However, the measurements (temperature, velocity and pollutant concentration) of selected locations can be used to compare with the prediction of the theoretical and reduced-scale models. Another reason for using several methods is that the structure of flow in the urban canopy is different to most types of turbulent flows -because in this case the large eddies penetrate through the whole shear layer and reinforce the internal shear layer. But different aspects of these complex flows come from the different modelling, measurement and simulations. The other point is that new lab and field measurements are enabling the mechanisms to be identified.

We have seen that the formation of BTDAC generally occurs over urban heat island areas during calm background weather conditions. The main features of the flow are convergent inflow, divergent outflow and upward flow at the urban centre. However, the detailed three-dimensional structure of BTDAC is also important both locally, such as in building-area density, building height variation, *etc.*, and more significantly in differently formed (*e.g.*, circular or star shaped) zonal areas with different surface properties (*e.g.*, inner city, suburban, green areas, *etc.*). As proposed by Fan et al. (2016a), the influence of the aspect ratio (the ratio of the urban diameter to the mixed height) must also be explored.

The pollutants emitted in the BTDAC covered region depend on the scale and flow structure (as explained above). Given the horizontal extension of the BTDAC of 30 km and the mean circulation speed of 2 m/sec, the time scale of total mixing is about 4 hr. Based on the study of Sells and Hay (1973), thermals and smaller scale plumes both exist in BTDAC, depending on the urban morphology (road size, building size, district size) and heating load distribution in the urban area. The upward velocities within thermals are generally greater than the mean city-scale plume circulation, which enhances the vertical mixing process. If the BTDAC is assumed to be steady and approximately symmetrical, how rapidly do the pollutants disperse around the axis of the symmetry? The dispersion is also affected by the large shear between the inflow and the outflow, which according to Hunt and Durbin (1999), tends to block the weaker thermals as they rise through the intermediate shear region in the centre of the mixed layer.

5. Conclusions

In this paper, the characteristics of BTDAC and, in the absence of a significant approach wind, the mechanisms of an idealised BTDAC formation are reviewed and discussed. BTDAC is an important focus of research on the urban climate and plays a crucial role in urban ventilation and pollutant dispersion. Various methods of investigating BTDAC are available, such as mathematical models, numerical simulations, field measurements, reduced-scale air-tank models and reduced-scale water-tank models. Air-tank models have been less frequently used in recent years, probably due to the discrepancy between the results of such models and real atmospheric data. Water-tank models offer a substitute method, proven to simulate BTDAC with ease, efficiency and precision. BTDAC is a transient process, and can interact with BTDAC generated in nearby cities. Some of the characteristics of BTDAC differ between day and night. The detailed process of pollutant mixing within BTDAC and the interaction of different areas of BTDAC offer interesting topics of future research, as city clusters continue to grow in many parts of the world.

The modelling of flow and dispersion in urban areas also depends on steady and unsteady mesoscale modelling and data in synoptic conditions outside large urban areas, such as cold fronts and sandstorms, to predict when rapid ventilation and improvements of polluted air can and will occur (*e.g.*, Wehner et al., 2004). The formation of BTDAC can, as discussed, lead to the rapid accumulation of pollutants or an 'explosive growth' of the haze. Sudden changes in wind pattern and/or a slight rise in the approach wind can lead to a sudden change in wind pattern and a significant increase in ventilation (*e.g.*, Liu et al., 2013; Wang et al., 2014). Planners should also consider that beneficial wind patterns can be artificially established when planning or altering cities to produce asymmetrical patterns of groups of buildings, infrastructure or green spaces with different thermal or aerodynamic properties, or perhaps in controlling traffic flow to optimise dispersion (Fan et al., under review).

Acknowledgment

This work is supported financially by a RGC CRF project (HKU9/CRF/12G) of the Hong Kong SAR Government. JH is grateful for support from the Newton Ungku Omar fund administered by the British Council and the Malaysian International Group for High Technology. We are grateful for input from J Stocker and DJ Carruthers of CERC Ltd., and Dr. Yasemin Akhtas of the Civil Engineering Department, UCL.

REFERENCES

Banta, R.M., Senff, C.J., White, A.B., Trainer, M., McNider, R.T., Valente, R.J., Mayor, S.D., Alvarez, R.J., Hardesty, R.M., Parrish, D., Fehsenfeld, F.C., 1998. Daytime buildup and nighttime

transport of urban ozone in the boundary layer during a stagnation episode. J. Geophys. Res.-Atmos. (1984–2012) 103, 22519–22544.
Barlag, A.-B., Kuttler, W., 1991. The significance of country breezes for urban planning. Energ. Buildings 15, 291–297.
Bohnenstengel, S.I., Evans, S., Clark, P.A., Belcher, S.E., 2011. Simulations of the London urban heat island. Q. J. R. Meteorol. Soc. 137 (659), 1625–1640.
Catalano, F., Cenedese, A., Falasca, S., Moroni, M., 2012. Numerical and experimental simulations of local winds. In: Fernando, H.J.S., et al. (Eds.), National Security and Human Health Implications of Climate Change. Springer, Netherlands, pp. 199–218.
Cenedese, A., Monti, P., 2003. Interaction between an inland urban heat island and a sea-breeze flow: a laboratory study. J. Appl. Meteorol. 42, 1569–1583.
Cheng, C., Chan, J.C.L., 2012. Impacts of land use changes and synoptic forcing on the seasonal climate over the Pearl River Delta of China. Atmos. Environ. 60, 25–36.
Eliasson, I., 2000. The use of climate knowledge in urban planning. Landsc. Urban Plan. 48, 31–44.
Eliasson, I., Holmer, B., 1990. Urban heat island circulation in Göteborg, Sweden. Theor. Appl. Climatol. 42, 187–196.
Falasca, S., Moroni, M., Cenedese, A., 2013. Laboratory simulations of an urban heat island in a stratified atmospheric boundary layer. J. Vis. Jpn. 16, 39–45.
Fan, Y., Li, Y., Wang, X., Catalano, F., 2016a. A new convective velocity scale for studying diurnal urban heat island circulation. J. Appl. Meteorol. Climatol. 55, 2151–2164.
Fan, Y., Hunt, J.C.R., Yin, S., Li, Y., 2016b. The plume-puff eddy structure and mean shear flow in recirculating turbulent urban convection below stably stratified inversion layers. Bound.-Layer Meteorol. (under review).
Fernando, H.J.S., Lee, S.M., Anderson, J., Princevac, M., Pardyjak, E., Grossman-Clarke, S., 2001. Urban fluid mechanics: air circulation and contaminant dispersion in cities. Environ. Fluid Mech. 1, 107–164.
Findlay, B., Hirt, M., 1969. An urban-induced meso-circulation. Atmos. Environ. (1967) 3, 537–542.
Ganbat, G., Baik, J.-J., Ryu, Y.-H., 2014. A numerical study of the interactions of urban breeze circulation with mountain slope winds. Theor. Appl. Climatol. 120, 123–135.
Han, J.-Y., Baik, J.-J., 2009. Theoretical studies of convectively forced mesoscale flows in three dimensions. Part I: uniform basic-state flow. J. Atmos. Sci. 66, 947–965.
Hidalgo, J., Masson, V., Pigeon, G., 2008a. Urban-breeze circulation during the CAPITOUL experiment: numerical simulations. Meteorog. Atmos. Phys. 102, 243–262.
Hidalgo, J., Pigeon, G., Masson, V., 2008b. Urban-breeze circulation during the CAPITOUL experiment: observational data analysis approach. Meteorog. Atmos. Phys. 102, 223–241.
Hidalgo, J., Masson, V., Gimeno, L., 2010. Scaling the daytime urban heat island and urban-breeze circulation. J. Appl. Meteorol. Climatol. 49, 889–901.
Hunt, J.C.R., 2005. London's Environment: Prospects for a Sustainable World City. Imperial College Press, London.
Hunt, J.C.R., Durbin, P.A., 1999. Perturbed vortical layers and shear sheltering. Fluid Dyn. Res. 24, 375–404.
Hunt, J.C.R., Simpson, J.E., 1982. Atmospheric boundary layers over non-homogeneous terrain. In: Plate, E.J. (Ed.), Chapter 7 of 'Engineering Meteorology'. Elsevier, New York, pp. 269–318.
Hunt, J.C.R., Vrieling, A.J., Nieuwstadt, F.T.M., Fernando, H.J.S., 2003. The influence of the thermal diffusivity of the lower boundary on eddy motion in convection. J. Fluid Mech. 491, 183–205.
Hunt, J.C.R., Orr, A., Rottman, J.W., Capon, R., 2004. Coriolis effects in mesoscale flows with sharp changes in surface conditions. Q. J. R. Meteorol. Soc. 130 (603), 2703–2731.
Hunt, J.C.R., Pacheco, J.R., Mahalov, A., Fernando, H.J.S., 2005. Effects of rotation and sloping terrain on fronts of density current fronts. J. Fluid Mech. 537, 285–315.
Hunt, J.C.R., Bohnenstengel, S., Belcher, S.E., Timoshkina, Y., 2012. Implications of climate change for expanding cities worldwide. Proc. Inst. Civ. Eng. – Urban Des. Plann. 166, 241–254.
Hunt, J.C.R., Chan, J.C.L., Wu, J., 2016. Asian urban environment and climate change. Curr. Sci. India 10, 1398–1400.
Kristóf, G., Rácz, N., Balogh, M., 2009. Adaptation of pressure based CFD solvers for mesoscale atmospheric problems. Bound.-Layer Meteorol. 131, 85–103.
Lemonsu, A., Masson, V., 2002. Simulation of a summer urban breeze over Paris. Bound.-Layer Meteorol. 104, 463–490.
Liang, M., Keener, T.C., 2015. Atmospheric feedback of urban boundary layer with implications for climate adaptation. Environ. Sci. Technol. 49, 10598–10606.
Liu, X.G., Li, J., Qu, Y., Han, T., Hou, L., Gu, J., Zhang, Y., 2013. Formation and evolution mechanism of regional haze: a case study in the megacity Beijing, China. Atmos. Chem. Phys. 13 (9), 4501–4514.
Long, S., Zhu, Y., Jang, C., Lin, C.-J., Wang, S., Zhao, B., Gao, J., Deng, S., Xie, J., Qiu, X., 2016. A case study of development and application of a streamlined control and response modeling system for $PM_{2.5}$ attainment assessment in China. J. Environ. Sci. 41, 69–80.
Lu, J., Arya, S.P., Snyder, W.H., Lawson Jr., R.E., 1997a. A laboratory study of the urban heat island in a calm and stably stratified environment. Part I: temperature field. J. Appl. Meteorol. 36, 1377–1391.
Lu, J., Arya, S.P., Snyder, W.H., Lawson Jr., R.E., 1997b. A laboratory study of the urban heat island in a calm and stably stratified environment. Part II: velocity field. J. Appl. Meteorol. 36, 1392–1402.
Luo, Z., Li, Y., 2011. Passive urban ventilation by combined buoyancy-driven slope flow and wall flow: parametric CFD studies on idealized city models. Atmos. Environ. 45, 5946–5956.
Masson, V., Gomes, L., Pigeon, G., Liousse, C., Pont, V., Lagouarde, J.-P., Voogt, J., Salmond, J., Oke, T., Hidalgo, J., 2008. The canopy and aerosol particles interactions in Toulouse urban layer (CAPITOUL) experiment. Meteorog. Atmos. Phys. 102, 135–157.
Miao, Y., Liu, S., Zheng, Y., Wang, S., Chen, B., Zheng, H., Zhao, J., 2015. Numerical study of the effects of local atmospheric circulations on a pollution event over Beijing–Tianjin–Hebei, China. J. Environ. Sci. 30, 9–20.
Mori, A., Niino, H., 2002. Time evolution of nonlinear horizontal convection: its flow regimes and self-similar solutions. J. Atmos. Sci. 59, 1841–1856.
Moroni, M., Cenedese, A., 2015. Laboratory simulations of local winds in the atmospheric boundary layer via image analysis. Adv. Meteorol. 2015, 618903.
Noto, K., 1996. Dependence of heat island phenomena on stable stratification and heat quantity in a calm environment. Atmos. Environ. 30, 475–485.
Noto, K., Okamoto, H., 1991. Thermal plume from a heat source in thermally stable stratified air: fundamental characteristics of heat island phenomenon. Energ. Buildings 15, 183–190.
Parkhi, N., Chate, D., Ghude, S.D., Peshin, S., Mahajan, A., Srinivas, R., Surendran, D., Ali, K., Singh, S., Trimbake, H., Beig, G., 2016. Large inter annual variation in air quality during the annual festival 'Diwali' in an Indian megacity. J. Environ. Sci. 43, 265–272.
Ryu, Y.H., Baik, J.-J., Han, J.Y., 2013. Daytime urban breeze circulation and its interaction with convective cells. Q. J. R. Meteorol. Soc. 139, 401–413.
Sells, V., Hay, D., 1973. Lidar evidence of thermal plumes in an urban environment. Atmosphere 11, 162–165.
Shreffler, J.H., 1979. Heat island convergence in St. Louis during calm periods. J. Appl. Meteorol. 18, 1512–1520.

Sini, J.-F., Anquetin, S., Mestayer, P.G., 1996. Pollutant dispersion and thermal effects in urban street canyons. Atmos. Environ. 30, 2659–2677.
Snyder, W.H., 1981. Guideline for fluid modeling of atmospheric diffusion. Tech. Rep. Environmental Protection Agency, Research Triangle Park, NC, USA.
Turfus, C., 1986. Diffusion from a continuous source near a surface in steady reversing shear flow. J. Fluid Mech. 172, 183–209.
Turfus, C., 1988. Calculating mean concentrations for steady sources in recirculating wakes by a particle trajectory method. Atmos. Environ. (1967) 22 (7), 1271–1290.
Vukovich, F.M., 1971. Theoretical analysis of the effect of mean wind and stability on a heat island circulation characteristic of an urban complex. Mon. Weather Rev. 99, 919–926.
Wang, X., Li, Y., 2016. Predicting urban heat island circulation using CFD. Build. Environ. 99, 82–97.
Wang, L., Zhang, N., Liu, Z., Sun, Y., Ji, D., Wang, Y., 2014. The influence of climate factors, meteorological conditions, and boundary-layer structure on severe haze pollution in the Beijing-Tianjin-Hebei region during January 2013. Adv. Meteorol. 2014, 685971.
Wang, H., Zhu, Y., Jang, C., Lin, C.-J., Wang, S., Fu, J.S., Gao, J., Deng, S., Xie, J., Ding, D., Qiu, X., Long, S., 2015. Design and demonstration of a next-generation air quality attainment assessment system for $PM_{2.5}$ and O_3. J. Environ. Sci. 29, 178–188.
Wehner, B., Wiedensohler, A., Tuch, T.M., Wu, Z.J., Hu, M., Slanina, J., Kiang, C.S., 2004. Variability of the aerosol number size distribution in Beijing, China: new particle formation, dust storms, and high continental background. Geophys. Res. Lett. 31 (22), L22108.
Xie, B., Hunt, J.C.R., Carruthers, D.J., Fung, J.C.H., Barlow, J.F., 2013. Structure of the planetary boundary layer over Southeast England: modeling and measurements. J. Geophys. Res.-Atmos. 118 (14), 7799–7818.
Yin, Q., Wang, J., Hu, M., Wong, H., 2016. Estimation of daily $PM_{2.5}$ concentration and its relationship with meteorological conditions in Beijing. J. Environ. Sci. 48, 161–168.
Yoshikado, H., 1992. Numerical study of the daytime urban effect and its interaction with the sea breeze. J. Appl. Meteorol. 31, 1146–1164.
Zhu, Y., Lao, Y., Jang, C., Lin, C.-J., Xing, J., Wang, S., Fu, J.S., Deng, S., Xie, J., Long, S., 2015. Development and case study of a science-based software platform to support policy making on air quality. J. Environ. Sci. 27, 97–107.